Information Sciences Letters
An International Journal

http://dx.doi.org/10.18576/isl/100102

Modeling of Diffusive Patterns in Predator–Prey System using Turing Instability and Amplitude Equations

Teekam Singh[1], *Ramu Dubey*[2], *Vishnu Narayan Mishra*[3,*] *and Mahmoud Abdel-Aty*[4]

[1]Department of Mathematics, Graphic Era Hill University, Society Area, Clement Town, Dehradun 248002, India
[2]Department of Mathematics, J C Bose University of Science & Technology, Faridabad-121006, India
[3]Department of Mathematics, Indira Gandhi National Tribal University, Amarkantak-484887, India
[4]Department of Mathematics, Faculty of Science, Sohag University, 82524 Sohag, Egypt

Received: 2 Sep. 2020, Revised: 11 Oct. 2020, Accepted: 10 Nov. 2020
Published online: 1 Jan. 2021

Abstract: In this work, we have investigated the evolution of diffusive pattern formation in a predator–prey model under type-III functional response. Using stability analysis, we receive the significant specifications for Turing instability (diffusive-driven instability), and with the help of these conditions, recognize the corresponding realm in the region of interest. Moreover, we present a qualitative analysis of growth and development actions that involves species distribution and their interplay of the spatially distributed populace with diffusion and obtain the conditions for spatial patterns like spots, spot-stripe, and stripes. Using weakly nonlinear analysis, we derive the equations of amplitude for slow modulation near the Turing boundary. By the series of numerical simulations, we receive intricate spatial patterns, particularly spot, stripe, and spot-stripe in the Turing realm. The consequences of this paper are general in the real world and can be used to investigate the impact of self-diffusion on other predator–prey systems. It will improve our understanding to understand the dynamical behavior of realistic models..

Keywords: Predator–prey system, hunting cooperation, diffusive patterns, Turing instability, amplitude equations

1 Introduction

Diffusion-driven spatial patterns in the natural world are universal, with examples such as stripes on zebra skin, diffusive–driven patterns in a quantum field, or Turing patterns in predator–prey systems [1–3]. Diffusive–driven components of populations interplay has been identified as a essential factor in how biological communities are formed and biological interplay occur over a wide limit of non-spatial and spatiotemporal scale [4]. Population distribution is of major significance in the study of biological models [5–7]. The distribution of diffusive populace is affected by the proliferation power of the populace and interplays among biological individuals [8]. The effect of diffusion may be ignored in a certain level, especially when the populace of a given species stays fixed in space at any moment of time. Albeit this assumption is not completely realistic. Individuals of an ecological species do not fixed at all times in space, and their dispersion in space changes incessantly by the self-movement of individuals [2, 5, 9–11].

Spatiotemporal modeling is a proper mechanism for investigating the elementary properties of complex population dynamical systems. A proper mathematical organization to clarify the dynamical behavior of diffusive phenomenon of biological population is specified by partial differential equations (reaction–diffusion system). Diffusion–Reaction models were primarily applied to depict the biological diffusive pattern development by Segel and Jackson in 1972, based on the initial research work of Alan M. Turing [12]. Over the past few years, large number of research paper have been published on the diffusive patterns dynamics of predator–prey system based on reaction–diffusion equations, and distinct kinds of patterns have emerged from these systems [2, 3, 5, 9–12].

Idea of diffusion may be considered as the natural propensity for a cluster of particles at the beginning concentrated close to a location in space to spread out in time, slowly occupying an ever sizable area close to the initial point. Here, the word “particles” mention not only to physical portion of the matter, but to biological

* Corresponding author e-mail: vishnunarayanmishra@gmail.com

populations or to any other recognizable elements as well. Moreover, the word "space" does not mention only to general Euclidean n-space but can also be an hypothetical living space (such as ecological space) [2, 5, 10]. Diffusion is a natural phenomenon where the movement of physical material from high concentration to low concentration space, that is, diffusion is a natural process by which the particle cluster as an entire dispersions according to the non-uniform movement of every particle. Diffusion can be defined to be basically an invariant process by which particle clusters, population, etc., diffuse inside a given space according to individual random movement [10].

Diffusion-Reaction partial differential equation systems can be used to represent mathematical models, which describe how the individuals of one or more species distributed in space changes under the effect of two procedures, first is local interaction, in which the species interact with each other, and second is the diffusion, which causes the species to spread out over a surface in space. Mathematically, reaction-diffusion systems take the form of semi-linear parabolic partial differential equations [5, 10, 11].

Through mathematical modeling as a viable tool, complex biological processes are studied. Mathematical modeling can be extremely helpful in analyzing factors that may contribute to the complexity intrinsic in insufficiently understood tumor–immune as well as predator–prey interactions. Likewise, the primary objective of the mathematical modeling of tumor–immune and Predator–prey models are, briefly, the analysis of the interplay inside and between biological species and their artificial surrounding, and the examination of the temporal transformation of clusters of individuals of different biological species. It is however true that space and time are indivisible "sibling co-ordinates" and only when population densities (tumor–immune system or predator–prey system) are contemplated in both space and time, actual dynamics can be understood [5, 6, 13–18].

Cooperative conduct can animate a association among the density of populace and per capita populace development rate [19, 20]. Environmentalists have recognized the few components for invigorating helpful conduct in prey, in particular supporting reproduction, searching efficiency, etc. Cooperative conduct in prey might be created by predation or by method natural to the prey life expectancy history [21]. Large number of research publications have been published to cooperative behavior in preys [22–27] and cooperative conduct is comparatively less analyzed in predators and poorly accepted [28–30], specifically when spatial behavior of population is considered clearly. Temporal model of predator–prey interaction under cooperative behavior through the simultaneous ordinary differential equation has been studied by Alves et.al. [31]. Influenced by their research work, we alter and expand the model in a spatial area to contemplate its spatial pattern formation.

Most of the models in mathematical ecology or tumor–immune interaction deal with non-spatial variant. The rate of change of the number of individuals u in a population may be manifested as the derivative with respect to time 't', du/dt. The model equations of a biological community of interacting individuals and their environment are then founded by equating this derivative to another relation expressing the effect of species interaction on population. Same is the situation with tumor–immune interacting models. This type of straightforward analysis is not practicable when spatial models are considered. Directly connected to species interplay is the net population via an arbitrary infinitesimal piece of space rather than the spatial rate of change of the population itself, and thus a reasonable manifestation is unreachable without knowledge of the mechanism of motion of the individuals.

This research work is structured as: We developed a reaction–diffusion predator–prey model with hunting cooperation in predators with zero-flux boundary conditions and non-zero initial population distribution in Section 2. Furthermore, we studied the non-spatial dynamical behavior of the model with hunting cooperation in predators for local stability investigation in Section 3. In Section 4, we get the adequate conditions for Turing bifurcation with Neumann's condition. We have derived the amplitude equations via weakly nonlinear analysis in Section 5. In Section 6, we use numerical simulations to validate the theoretical results obtained in the previous sections. The paper ends with a discussion 7.

2 Mathematical model

By including the spatial aspect and type III functional response in the extensive predator–prey system with hunting cooperation [31, 32], we obtain the following predator–prey system

$$\begin{aligned}\frac{dX}{dt'} &= \left(1-\frac{X}{K}\right)rX - \frac{(\lambda+aY)X^2Y}{1+H_1(\lambda+aY)X^2}\\ \frac{dY}{dt'} &= e\frac{(\lambda+aY)X^2Y}{1+H_1(\lambda+aY)X^2} - mY.\end{aligned} \tag{1}$$

Here the masses of prey and predator population at time t' are represented by $X(t')$ and $Y(t')$, serially. r is rate of natural growth of prey, K is its holding efficiency, λ is the constant invasion rate, and a is the rate of predator hunting cooperation. e parameter represent the efficiency of transition, and m is the predator's natural mortality rate. H_1 is the handling time of predator. All parameters are positive.

On the contrary, we presume that the prey and predator populace densities spread without any order and this random distribution of species is depicted by diffusion. Then, we propose a spatial predator–prey model with hunting cooperation and Allee effects in

predators corresponding to (1) as follows:

$$\frac{\partial X}{\partial t'} = \left(1-\frac{X}{K}\right)rX - \frac{(\lambda+aY)X^2Y}{1+H_1(\lambda+aY)X^2} + d_1\nabla^2 X$$
$$\frac{\partial Y}{\partial t'} = e\frac{(\lambda+aY)X^2Y}{1+H_1(\lambda+aY)X^2} - mY + d_2\nabla^2 Y \quad (2)$$

where d_1 and d_2 are the non-negative diffusion coefficients of prey and predator, respectively. ∇^2 is the usual Laplacian operator in $d \leq 3$ space dimensions.

Presently we non-dimensionalize the system (2) by presenting the following dimensionless factors

$$t = mt', \quad u = x\sqrt{\frac{e\lambda}{m}}, \quad v = Y\sqrt{\frac{\lambda}{me}},$$

and dimensionless values of other parameters are given by

$$\sigma = \frac{r}{m}, \quad N = \sqrt{\frac{e\lambda}{m}}K, \quad \alpha = \frac{a}{\lambda}\sqrt{\frac{em}{\lambda}}, \quad h_1 = \frac{m}{e}H_1.$$

With these changes, Eqs. (2) become

$$\frac{\partial u}{\partial t} = \left(1-\frac{u}{N}\right)\sigma u - \frac{(1+\alpha v)u^2 v}{1+h_1(1+\alpha v)u^2} + d_1\nabla^2 u$$
$$\frac{\partial v}{\partial t} = \frac{(1+\alpha v)u^2 v}{1+h_1(1+\alpha v)u^2} - v + d_2\nabla^2 v. \quad (3)$$

This is the working spatial predator–prey model with hunting cooperation and Allee effects in predators. Generally, to make effective that diffusive patterns are ruled by Turing instability method, model 3 is to be investigated with the following initial conditions:

$$2D: u(x,y,0) > 0, \;\; v(x,y,0) > 0, \;\; (x,y) \in \Omega = [0,L]\times[0,L] \quad (4)$$

and Neumann's boundary condition

$$\frac{\partial u}{\partial \nu} = \frac{\partial v}{\partial \nu} = 0, \quad (5)$$

where L is the size of the homogeneous spatial domain, ν is the unit normal on the boundary $\partial\Omega$. Neumann boundary condition (zero-flux) (5) insinuate that no biological population leave the simulation space.

3 Analysis of the Temporal Model

3.1 Initial Density Distribution

The spatiotemporal pattern formation generally onset with a community interplays of species. The initial conditions for model (3) should be stated by the mathematical compact support function that is within a definite region the initial density distribution of prey and predator is non-zero and elsewhere zero. The structure of the realm and the outlines of the species densities can be dissimilar in different predator–prey models. In this study, we have employed the positive initial distribution of species in space as

$$u(x_i,y_j,0) = u^* + \gamma_1\varepsilon_{ij},$$
$$v(x_i,y_j,0) = v^* + \gamma_2\eta_{ij}, \quad (6)$$

where γ_1 and γ_2 are small reals and ε_{ij} and η_{ij} are white Gaussian noise with certain variance and zero mean.

3.2 Equilibria of System

Without diffusion the steady states equilibria of the model are given by

$$\left(1-\frac{u}{N}\right)\sigma u - \frac{(1+\alpha v)u^2 v}{1+h_1(1+\alpha v)u^2} = 0,$$
$$\frac{(1+\alpha v)u^2 v}{1+h_1(1+\alpha v)u^2} - v = 0. \quad (7)$$

Clearly the above system has the following meaningful steady state points: (i) $E_0(0,0)$ (prey and predator both extinct), (ii) $E_1(N,0)$ (prey only survive) and (iii) two positive coexistence equilibrium points $E_2(u_2,v_2)$ and $E_3(u_3,v_3)$ (interior equilibrium solutions), where $v_2 = \frac{1}{\alpha}\left(\frac{1}{(1-h_1u_2)u_2} - 1\right)$ and $v_3 = \frac{1}{\alpha}\left(\frac{1}{(1-h_1u_3)u_3} - 1\right)$, and u_2, u_3 be the positive solution of

$$A_0u^4 + A_1u^3 + A_2u^2 + A_3u + A_4 = 0, \quad (8)$$

where
$A_0 = h_1\alpha\sigma$, $A_1 = (h_1N-1)\alpha\sigma$, $A_2 = ((1-h_1)\alpha\sigma - h_1)N$, $A_3 = (1-h_1)N$, $A_4 = -N$.

The number of coexistence equilibrium points and their stability depends upon the parameter values for the model (3).

3.3 Stability Analysis of System

The Jacobian matrix (**J**) of the model of (3) is as follows

$$\begin{bmatrix} \Delta_{11} & \Delta_{12} \\ \Delta_{21} & \Delta_{22} \end{bmatrix} = (\Delta_{ij})_{2\times 2}, \quad (9)$$

where

$$\Delta_{11} = \sigma\left(1-\frac{2u}{N}\right) + \frac{v(1+v\alpha)[(1+v\alpha)h_1u^2-1]}{[1+(1+v\alpha)h_1u+(1+v\alpha)h_1u^2]^2},$$
$$\Delta_{12} = -\frac{u[1+2\alpha v+(1+\alpha v)^2h_1u+(1+\alpha v)^2h_1u^2]}{[1+(1+\alpha v)h_1u+(1+\alpha v)h_1u^2]^2},$$
$$\Delta_{21} = -\frac{v(1+v\alpha)[(1+v\alpha)h_1u^2-1]}{[1+(1+v\alpha)h_1u+(1+v\alpha)h_1u^2]^2},$$
$$\Delta_{22} = \frac{u[1+2\alpha v+(1+v\alpha)^2h_1u+(1+v\alpha)^2h_1u^2]}{[1+(1+v\alpha)h_1u+(1+v\alpha)h_1u^2]^2} - 1.$$

1.At $E_0(0,0)$, Jacobian matrix is

$$\mathbf{J}_0 = \begin{bmatrix} \sigma & 0 \\ 0 & -1 \end{bmatrix},$$

whose eigenvalues are -1 and σ (which is a positive parameter). Therefore the model (3) is not stable at the $(0,\ 0)$.

2.At $E_1(N,0)$, Jacobian matrix is

$$\mathbf{J}_1 = \begin{bmatrix} -\sigma & -\frac{N}{1+h_1N+h_1N^2} \\ 0 & \frac{N}{1+h_1N+h_1N^2} - 1 \end{bmatrix},$$

whose eigenvalues are $-\sigma$ and $\frac{N}{1+h_1N+h_1N^2} - 1$. Hence the system is locally asymptotically stable if $\frac{N}{1+h_1N+h_1N^2} < 1$.

3.At $E_2(u_2, v_2)$

Lemma 1. The equilibrium solution $E_2(u_2, v_2)$ is locally asymptotically stable if and only if

$$(N - N\sigma + 2\sigma u_2)(1 + h_1u_2(1 + v_2\alpha) + h_1{u_2}^2(1 + v_2\alpha))^2 - N(u_2(1+2\alpha v_2) - v_2(1+\alpha v_2) + (h_1u_2 + h_1v_2 + h_1)(1+\alpha v_2)^2{u_2}^2) > 0,$$

and

$$u_2v_2(1 + \alpha v_2)(1 - h_1{u_2}^2(1 + \alpha v_2))N(1 + 2\alpha v_2 + h_1u_2(1+\alpha v_2)^2 + h_1u_2(1+\alpha v_2)^2) + (-(1 + h_1{u_2}^2(1 + \alpha v_2) + h_1u_2(1 + \alpha v_2))^2 + u_2(1 + 2\alpha v_2 + h_1u_2(1 + \alpha v_2)^2 + h_1{u_2}^2(1 + \alpha v_2)^2))(v_2(1 + \alpha v_2)N(-1 + h_1{u_2}^2(1+\alpha v_2)) - 2\sigma u_2(1 + h_1u_2(1+\alpha v_2) + h_1{u_2}^2(1 + \alpha v_2))^2 + \sigma N(1 + h_1u_2(1+\alpha v_2) + h_1{u_2}^2(1+\alpha v_2))^2) > 0.$$

Proof 1. The eigenvalues of the corresponding Jacobian matrix $\mathbf{J}$ at equilibrium solution $E_2(u_2, v_2)$ are given by $\frac{1}{2}(\mu_1 \pm \mu_2)$, where

$$\mu_1 = \sigma(1 - \frac{2u_2}{N}) - 1 + \frac{v_2(1+\alpha v_2)(h_1{u_2}^2(1+\alpha v_2) - 1)}{(1 + h_1u_2(1+\alpha v_2) + h_1{u_2}^2(1+\alpha v_2))^2} + \frac{u_2(1+2\alpha v_2 + h_1u_2(1+\alpha v_2)^2 + h_1{u_2}^2(1+\alpha v_2)^2)}{(1+h_1u_2(1+\alpha v_2) + h_1{u_2}^2(1+\alpha v_2))^2},$$

$\mu_2 = \sqrt{{\mu_1}^2 - 4\mu_3}$ and μ_3 is the determinant of Jacobian $\mathbf{J}$ at $E_2(u_2, v_2)$. Hereby, the coexistence equilibrium solution $E_2(u_2, v_2)$ is locally asymptotically stable if and only if $\mu_1 < 0$ and $\mu_3 < 0$.

Lemma 2. The reaction-diffusion system (3) enters into a Hopf-bifurcation around $E_2(u_2, v_2)$ at $\sigma = \sigma_{hb}$, where σ_{hb} satisfies the equality

$$\sigma_{hb} = \frac{N((1+h_1u_2(1+\alpha v_2) + h_1{u_2}^2(1+\alpha v_2))^2 - u_2(1+2\alpha v_2)}{(N-2u_2)(1+h_1u_2(1+\alpha v_2) + h_1{u_2}^2(1+\alpha v_2))^2} - \frac{(h_1 + v_2h_1 + u_2h_1)(1+\alpha v_2)^2{u_2}^2)}{(N-2u_2)(1+h_1u_2(1+\alpha v_2) + h_1{u_2}^2(1+\alpha v_2))^2}.$$

Proof 2. The characteristic equation corresponding to the equilibrium solution $E_2(u_2, v_2)$ is given by ${\lambda_{11}}^2 - \mu_1\lambda_{11} + \mu_3 = 0$. Let us assume that

$$u \approx \exp(\lambda_{11}t), \quad v \approx \exp(\lambda_{11}t).$$

If $\mu_1 = 0$, at that point both the eigenvalues will be simply imaginary given μ_3 is non-negative and there are no different eigenvalues with negative real part. Presently $\mu_1 = 0$ gives $\sigma = \sigma_{hb}$. Substituting $\lambda_{11} = a_1 + ib_1$ into the equation ${\lambda_{11}}^2 - \mu_1\lambda_{11} + \mu_3 = 0$ and separating real and imaginary parts we obtain $({a_1}^2 - {b_1}^2) - \mu_1a_1 + \mu_3 = 0$ and $2a_1b_1 - \mu_1b_1 = 0$. Differentiating $2a_1b_1 - \mu_1b_1 = 0$ both sides with respect to σ at $\sigma = \sigma_{hb}$ and considering $a_1 = 0$, we get

$$\left.\frac{da_1}{d\sigma}\right|_{\sigma=\sigma_{hb}} = \frac{1}{2}\left(1 - \frac{2u_2}{N}\right) \neq 0.$$

Now the bifurcation in stability about $E_2(u_2, v_2)$, we should have the real part of λ_{11}, that is, $a_1 = 0$. Hence, the system undergoes a Hopf-bifurcation at $E_2(u_2, v_2)$ as σ passes through the value σ_{hb}.

4 Analysis of the spatiotemporal model

Coexistence equilibria $E_2(u_2, v_2)$ of temporal model is spatially homogenous equilibria, i.e., fixed in simulated space and time for the diffusive system. Assumption for Turing instability is that the $E_2(u_2, v_2)$ is stable in temporal system that is the spatially uniform equilibrium is stable under spatially uniform perturbations. In spite of the fact that the dispersion is frequently consider as a balancing out procedure, this is a notable reality that spatially uniform equilibria become unstable using diffusion concerning non-uniform perturbations in a system of interacting populations [3, 12]. The stipulation for diffusive pattern formation may be attained by inserting a non-uniform perturbation of the uniform equilibria as

$$\begin{aligned} u(x,y,t) &= u_2 + \varepsilon_1 \exp(\lambda_k t)\cos(k_x x)\cos(k_y y), \\ v(x,y,t) &= v_2 + \varepsilon_2 \exp(\lambda_k t)\cos(k_x x)\cos(k_y y), \end{aligned} \tag{10}$$

where ε_1 and ε_2 are reals and $(k_x, k_y) = k$, such that $k^2 = \left(k_x^2 + k_y^2\right)$, is the number of waves in a unit distance.

Substituting (10) into (3) and then make linear it about coexistence equilibrium $E_2(u_2, v_2)$, we receive the Jacobian as

$$\begin{bmatrix} S_{11} & S_{12} \\ S_{13} & S_{14} \end{bmatrix}_{(u_2,v_2)},$$

where

$$S_{11} = \sigma(1 - \frac{2u_2}{N}) + \frac{v_2(1+v_2\alpha)[(1+v_2\alpha)h_2u_2^2 - 1]}{[1 + (1+v_2\alpha)h_1u_2 + (1+v_2\alpha)h_2u_2^2]^2} - k^2,$$

$$S_{12} = -\frac{u_2[1 + 2\alpha v_2 + (1+\alpha v_2)^2h_1u_2 + (1+\alpha v_2)^2h_1u_2^2]}{[1 + (1+\alpha v_2)h_1u_2 + (1+\alpha v_2)h_1u_2^2]^2},$$

$$S_{13} = -\frac{v_2(1+v_2\alpha)[(1+v_2\alpha)h_1u_2^2-1]}{[1+(1+v_2\alpha)h_1u_2+(1+v_2\alpha)h_1u_2^2]^2},$$
$$S_{14} = \frac{u_2[1+2\alpha v_2+(1+v_2\alpha)^2h_1u_2+(1+v_2\alpha)^2h_1u_2^2]}{[1+(1+v_2\alpha)h_1u_2+(1+v_2\alpha)h_1u_2^2]^2} - 1-dk^2, \quad d=\frac{d_2}{d_1}.$$

The corresponding characteristic equation is

$$\lambda^2 + C_1(k^2)\lambda + C_2(k^2) = 0, \tag{11}$$

where

$$C_1(k^2) = (1+d)k^2 + 1 + \sigma\Big(\frac{2u_2}{N} - 1\Big) - \frac{\alpha u_2v_2 + (1+\alpha v_2)\big(u_2 - v_2 + h_1{u_2}^3(1+\alpha v_2)\big)}{\big(1+h_1{u_2}^2(1+\alpha v_2)+h_1u_2(1+\alpha v_2)\big)^2} + \frac{(h_1+h_1v_2){u_2}^2\big(1+\alpha v_2\big)^2}{\big(1+h_1{u_2}^2(1+\alpha v_2)+h_1u_2(1+\alpha v_2)\big)^2},$$

$$C_2(k^2) = \frac{2(1+dk^2)u_2\big(1+{u_2}^4{h_1}^2(1+\alpha v_2)^2\big)\sigma + (1+dk^2)v_2N}{\big(1+h_1{u_2}^2(1+v_2\alpha)+h_1u_2(1+v_2\alpha)\big)^2N} + \frac{(k^2-\sigma)Nu_2\big(-1-2v_2\alpha+2h_1(1+dk^2)\big)+2\sigma h_1{u_2}^4}{\big(1+h_1{u_2}^2(1+v_2\alpha)+h_1u_2(1+v_2\alpha)\big)^2N} + \frac{2h_1N(1+dk^2)(k^2-\sigma)+2{u_2}^3(1+\alpha v_2)(2h_1(1+dk^2)}{\big(1+h_1{u_2}^2(1+v_2\alpha)+h_1u_2(1+v_2\alpha)\big)^2N} + \frac{{u_2}^3(1+\alpha v_2)h_1(-1+2h_1(1+dk^2))(1+\alpha v_2)(k^2-\sigma)N}{\big(1+h_1{u_2}^2(1+v_2\alpha)+h_1u_2(1+v_2\alpha)\big)^2N} + \frac{{u_2}^2(1+\alpha v_2)^2h_1+{u_2}^2{h_1}^2(1+dk^2)(1+\alpha v_2)(k^2-\sigma)}{\big(1+h_1{u_2}^2(1+v_2\alpha)+h_1u_2(1+v_2\alpha)\big)^2N}.$$

Using Routh-Hurwitz criterion, the model (3) will be linearly stable about $\mathrm{E}_2(u_2,v_2)$ if $C_1(k^2) > 0$ and $C_2(k^2) > 0$. Since d and k^2 both are positive and by the stability of the temporal system, $C_1(k^2) > 0$ is consistently positive. Hence, the stipulation for Turing bifurcation is $C_2(k^2) < 0$.

The polynomial function $C_2(k^2)$ has minimal for k, say k_{min}, where

$$k_{min}^2 = \frac{1}{2Nd(h_1+h_1u_2)\big(1+u_2(h_1+h_1u_2)(1+\alpha v_2)\big)^2} \times \Big(\big(-1-u_2(h_1+h_1u_2)-(-1+h_1+h_1u_2)(1+u_2)^2\big)N + d(h_1+h_1u_2)(v_2(1+\alpha v_2)\big(-1+h_1{u_2}^2(1+\alpha v_2)\big)-2\sigma \big(1+u_2(h_1+h_1u_2)(1+\alpha v_2)\big)^2+\sigma N\big(1+u_2(h_1+h_1u_2)\big)^2\Big).$$

For minimal k, diffusive-driven instability will take place when $C_2(k_{min}^2) < 0$. Therefore, substituting k_{min}^2 in $C_2(k^2)$, we obtain the stipulation for diffusive-driven instability as

$$d\Delta_{11} + \Delta_{22} - 2\sqrt{d}\sqrt{\Delta_{11}\Delta_{22}-\Delta_{12}\Delta_{21}} > 0 \tag{12}$$

The span of the wave-number for which diffusive-driven instability occur is (k_-,k_+) and in present span, we have $C_2(k^2) < 0$, where

$$k_- = \frac{d\Delta_{11}+\Delta_{22}-\sqrt{(d\Delta_{11}+\Delta_{22})^2-4d(\Delta_{11}\Delta_{22}-\Delta_{12}\Delta_{21})}}{2d},$$
$$k_+ = \frac{d\Delta_{11}+\Delta_{22}+\sqrt{(d\Delta_{11}+\Delta_{22})^2-4d(\Delta_{11}\Delta_{22}-\Delta_{12}\Delta_{21})}}{2d},$$

where the values of $\Delta_{ij},\ i,j=1,2$ are obtain from equation (9) about $\mathrm{E}_2(u_2,v_2)$.

5 Amplitude equations

The system changes very slow near to the Turing bifurcation value and slow modes become active modes. The study of the pattern formation of slow mode is possible by means of the amplitude equation. By weakly nonlinear analysis, we derived the amplitude equations and examine the diffusive patterns (e.g., spots, stripes, and spots-strips) by a system of three vital resonant classes of modes $(k_j,-k_j)$ $(j=1,2,3)$ making angle of $\frac{2\pi}{3}$ and $|k_j| = k_T$.

For obtaining the equation of amplitude, first linearize the given model (3) at steady state (u^*,v^*):

$$\frac{\partial}{\partial t}\begin{bmatrix}u\\v\end{bmatrix} = \begin{bmatrix}d_1\nabla^2u\\d_2\nabla^2v\end{bmatrix} + \begin{bmatrix}a_{11}&a_{12}\\a_{21}&a_{22}\end{bmatrix}\begin{bmatrix}u\\v\end{bmatrix} + \frac{1}{2}\begin{bmatrix}f_{uu}u^2+2f_{uv}uv+f_{vv}v^2\\g_{uu}u^2+2g_{uv}uv+g_{vv}v^2\end{bmatrix} + \frac{1}{6}\begin{bmatrix}f_{uuu}u^3+3f_{uuv}u^2v+3f_{uvv}uv^2+f_{vvv}v^3\\g_{uuu}u^3+3g_{uuv}u^2v+3g_{uvv}uv^2+g_{vvv}v^3\end{bmatrix}. \tag{13}$$

The solution of model (3), at close to onset can be expressed as

$$U = U_s + \sum_{j=1}^{3} U_0[A_j\exp(ik_j.r) + \bar{A}_j\exp(-ik_j.r)], \tag{14}$$

and

$$U^0 = \sum_{j=1}^{3} U_0[A_j\exp(ik_j.r) + \bar{A}_j\exp(-ik_j.r)], \tag{15}$$

where, U_s represent the uniform equilibrium state and U_0 is the characteristic-vector of linear operator. A_j and $\bar{A}_j$ (conjugate of A_j) represents the amplitude with modality k_j and $-k_j$ respectively. Using weakly nonlinear analysis the spatiotemporal evolution of the amplitudes A_j $(j=1,2,3)$ by the analysis of symmetries are given as

$$\tau_0\frac{\partial A_1}{\partial t} = \mu A_1 + h\bar{A}_2\bar{A}_3 - [g_1|A_1|^2 + g_2(|A_2|^2+|A_3|^2)]A_1,$$

$$\tau_0\frac{\partial A_2}{\partial t} = \mu A_2 + h\bar{A}_1\bar{A}_3 - [g_1|A_2|^2 + g_2(|A_1|^2+|A_3|^2)]A_2,$$

$$\tau_0 \frac{\partial A_3}{\partial t} = \mu A_3 + h\bar{A}_1\bar{A}_2 - [g_1|A_3|^2 + g_2(|A_1|^2 + |A_2|^2)]A_3, \tag{16}$$

where, τ_0 is the relaxation time and μ is the normalized distance to onset. Now we will get the exact but intricate expression of the coefficient τ_0, h, g_1, and g_2. The model (3) can be represented as

$$\frac{\partial U}{\partial t} = LU + N \tag{17}$$

where L and N are linear and nonlinear operators, respectively.

$$U = \begin{bmatrix} u \\ v \end{bmatrix}, \; L = \begin{bmatrix} a_{11} + d_1\nabla^2 & a_{12} \\ a_{21} & a_{22} + d_2\nabla^2 \end{bmatrix},$$

and

$$N = \begin{bmatrix} N_1 \\ N_2 \end{bmatrix} = \frac{1}{2}\begin{bmatrix} f_{uu}u^2 + 2f_{uv}uv + f_{vv}v^2 \\ g_{uu}u^2 + 2g_{uv}uv + g_{vv}v^2 \end{bmatrix} + \frac{1}{6}\begin{bmatrix} f_{uuu}u^3 + 3f_{uuv}u^2v + 3f_{uvv}uv^2 + f_{vvv}v^3 \\ g_{uuu}u^3 + 3g_{uuv}u^2v + 3g_{uvv}uv^2 + g_{vvv}v^3 \end{bmatrix}.$$

Near the Turing bifurcation value $d_2 = {d_2}^T$, we perturb d_2 by U in the perturbation ε as follows:

$$d_2 - {d_2}^T = \varepsilon {d_2}^1 + \varepsilon^2 {d_2}^2 + O(\varepsilon^3), \tag{18}$$

$$U = \begin{bmatrix} u \\ v \end{bmatrix} = \varepsilon \begin{bmatrix} u_1 \\ v_1 \end{bmatrix} + \varepsilon^2 \begin{bmatrix} u_2 \\ v_2 \end{bmatrix} + \varepsilon^3 \begin{bmatrix} u_3 \\ v_3 \end{bmatrix} + O(\varepsilon^4). \tag{19}$$

Substituting these expression into L we get

$$L = L_T + \varepsilon \begin{bmatrix} 0 & 0 \\ 0 & \nabla^2 \end{bmatrix} {d_2}^1 + \varepsilon^2 \begin{bmatrix} 0 & 0 \\ 0 & \nabla^2 \end{bmatrix} {d_2}^2 + O(\varepsilon^3), \tag{20}$$

where

$$L_T = \begin{bmatrix} a_{11} + d_1\nabla^2 & a_{12} \\ a_{21} & a_{22} + d_2\nabla^2 \end{bmatrix}. \tag{21}$$

Now we need to distribute the time scale for the system where each time scale T_i can be considered as an independent variable. By the derivative chain rule, the derivative concerning time should transfer into the following terms:

$$\frac{\partial}{\partial t} = \frac{\partial}{\partial T_0} + \varepsilon\frac{\partial}{\partial T_1} + \varepsilon^2\frac{\partial}{\partial T_2} + O(\varepsilon^3). \tag{22}$$

As the variable amplitude A is varying very slowly, therefore $\frac{\partial}{\partial T_0} = 0$. Then the above equation reduces to :

$$\frac{\partial}{\partial t} = \varepsilon\frac{\partial}{\partial T_1} + \varepsilon^2\frac{\partial}{\partial T_2} + O(\varepsilon^3). \tag{23}$$

According to different order of ε, expanding (23) as follows
For the first order of ε:

$$L_T \begin{bmatrix} u_1 \\ v_1 \end{bmatrix} = 0. \tag{24}$$

As L^T represents the linear operator at the $d_2 = {d_2}^T$. Now, we solve linear ε, we have

$$\begin{bmatrix} u_1 \\ v_1 \end{bmatrix} = \begin{bmatrix} x \\ 1 \end{bmatrix} [W_1 \exp(ik_1.r) + W_2 \exp(ik_2.r) + W_3 \exp(ik_3.r)] \tag{25}$$

where, the amplitude of $\exp(ik_j.r)$ is W_j, $|k_j| = {k_T}^*$ and its structure is established by the perturbation rate of higher order. For quadratic ε, we have

$$L_T \begin{bmatrix} u_2 \\ v_2 \end{bmatrix} = \frac{\partial}{\partial T_1}\begin{bmatrix} u_1 \\ v_1 \end{bmatrix} - \begin{bmatrix} 0 & 0 \\ 0 & {d_2}^2 \end{bmatrix}\nabla^2 \begin{bmatrix} u_1 \\ u_2 \end{bmatrix} - \frac{1}{2}\begin{bmatrix} f_{uu}{u_1}^2 + 2f_{uv}u_1v_1 + f_{vv}{v_1}^2 \\ g_{uu}{u_1}^2 + 2g_{uv}u_1v_1 + g_{vv}{v_1}^2 \end{bmatrix} = \begin{bmatrix} {F_u}^j \\ {F_v}^j \end{bmatrix}. \tag{26}$$

The vector capacity of the right-hand side of condition (26) must be orthogonal with zero characteristic-vector of operator ${L_T}^*$ to guarantee the presence of the non-zero solution of this condition. The trivial characteristic-vector of operator ${L_T}^*$ are

$$\begin{bmatrix} 1 \\ y \end{bmatrix} \exp(-ik_j.r) + c.c., \quad j = 1,2,3. \tag{27}$$

The orthogonality condition is

$$[1, y]\begin{bmatrix} {F_u}^j \\ {F_v}^j \end{bmatrix} = 0, \tag{28}$$

where F_u^j and F_v^j are the coefficient to $\exp(ik_j.r)$ term in F_u and F_v. Taking $\exp(ik_1.r)$, for example, we have

$$\begin{bmatrix} {F_u}^1 \\ {F_v}^1 \end{bmatrix} = \begin{bmatrix} x \\ 1 \end{bmatrix}\frac{\partial W_1}{\partial T_1} + \begin{bmatrix} 0 \\ {d_2}^1k^2 \end{bmatrix} W_1 - \begin{bmatrix} P \\ Q \end{bmatrix}\bar{W}_2\bar{W}_3, \tag{29}$$

where

$$P = f_{uu}{u_1}^2 + 2f_{uv}u_1v_1 + f_{vv}{v_1}^2,$$
$$Q = g_{uu}{u_1}^2 + 2g_{uv}u_1v_1 + g_{vv}{v_1}^2.$$

From the orthogonality condition, we can obtain the following results :

$$(x+y)\frac{\partial W_1}{\partial T_1} = -{k_T}^2{d_2}^1yW_1 + (P + yQ)\bar{W}_2\bar{W}_3,$$
$$(x+y)\frac{\partial W_2}{\partial T_1} = -{k_T}^2{d_2}^1yW_2 + (P + yQ)\bar{W}_1\bar{W}_3,$$
$$(x+y)\frac{\partial W_3}{\partial T_1} = -{k_T}^2{d_2}^1yW_3 + (P + yQ)\bar{W}_1\bar{W}_2.$$

Now solving condition (26), we have

$$\begin{bmatrix} u_2 \\ v_2 \end{bmatrix} = \begin{bmatrix} U_0 \\ V_0 \end{bmatrix} + \sum_{j=1}^{3}\begin{bmatrix} U_j \\ V_j \end{bmatrix}\exp(ik_j.r) + \sum_{j=1}^{3}\begin{bmatrix} U_{jj} \\ V_{jj} \end{bmatrix}\exp(i2k_j.r) + \begin{bmatrix} U_{12} \\ V_{12} \end{bmatrix}\exp[i(k_1 - k_2).r] + \begin{bmatrix} U_{23} \\ V_{23} \end{bmatrix}\exp[i(k_2 - k_3).r] + \begin{bmatrix} U_{31} \\ V_{31} \end{bmatrix}\exp[i(k_3 - k_1).r] + c.c\,. \tag{30}$$

Solution about $\exp(0)$, $\exp(ik_j.r)$, $\exp(i2k_j.r)$, and $\exp(i(k_j-k_k).r)$ of the above system of linear equations, we have

$$\begin{bmatrix}U_0\\V_0\end{bmatrix}=\begin{bmatrix}u_0\\v_0\end{bmatrix}(|W_1|^2+|W_2|^2+|W_3|^2),\ U_j=fV_j,$$

$$\begin{bmatrix}U_{jj}\\V_{jj}\end{bmatrix}=\begin{bmatrix}u_{11}\\v_{11}\end{bmatrix}W_j{}^2,\ \begin{bmatrix}U_{jk}\\V_{jk}\end{bmatrix}=\begin{bmatrix}u^*\\v^*\end{bmatrix}W_j\bar{W}_k,$$

where

$$\begin{bmatrix}u_0\\v_0\end{bmatrix}=\begin{bmatrix}a_{11}&a_{12}\\a_{21}&a_{22}\end{bmatrix}^{-1}\begin{bmatrix}-P\\-Q\end{bmatrix},$$

$$\begin{bmatrix}u_{11}\\v_{11}\end{bmatrix}=-\frac{1}{2}\begin{bmatrix}a_{11}-4k_T{}^2d_1&a_{12}\\a_{21}&a_{22}-4k_T{}^2d_2{}^T\end{bmatrix}^{-1}\begin{bmatrix}-P\\-Q\end{bmatrix},$$

$$\begin{bmatrix}u^*\\v^*\end{bmatrix}=-\begin{bmatrix}a_{11}-3k_T{}^2d_1&a_{12}\\a_{21}&a_{22}-3k_T{}^2d_2{}^T\end{bmatrix}^{-1}\begin{bmatrix}-P\\-Q\end{bmatrix}.$$

For third order of ε, we have

$$L_T\begin{bmatrix}u_3\\v_3\end{bmatrix}=\begin{bmatrix}\frac{\partial u_2}{\partial T_1}+\frac{\partial u_1}{\partial T_2}\\\frac{\partial v_2}{\partial T_1}+\frac{\partial v_1}{\partial T_2}\end{bmatrix}-\begin{bmatrix}0&0\\0&d_2{}^2\end{bmatrix}\nabla^2\begin{bmatrix}u_1\\v_1\end{bmatrix}-\begin{bmatrix}0&0\\0&d_2{}^1\end{bmatrix}\nabla^2$$
$$\times\begin{bmatrix}u_2\\v_2\end{bmatrix}-\frac{1}{2}\begin{bmatrix}f_{uu}u_1u_2+2f_{uv}(u_1v_2+u_2v_1)+2f_{vv}v_1v_2\\g_{uu}u_1u_2+2g_{uv}(u_1v_2+u_2v_1)+2g_{vv}v_1v_2\end{bmatrix}-$$
$$\frac{1}{6}\begin{bmatrix}f_{uuu}u_1{}^3+3f_{uuv}u_1{}^2v_1+3f_{uvv}u_1v_1{}^2+f_{vvv}v_1{}^3\\g_{uuu}u_1{}^3+3g_{uuv}u_1{}^2v_1+3g_{uvv}u_1v_1{}^2+g_{vvv}v_1{}^3\end{bmatrix}=\begin{bmatrix}G_u\\G_v\end{bmatrix}.$$

By the Fredholm solvability condition, we have

$$(x+y)\left(\frac{\partial V_1}{\partial T_1}+\frac{\partial W_1}{\partial T_2}\right)=-k_T{}^2y(d_2{}^2W_1+d_2{}^1V_1)+$$
$$h_1(\bar{W}_2\bar{V}_3+\bar{W}_3\bar{V}_2)+\bar{h_2}\bar{W}_2\bar{W}_3-(G_1|W_1|^2),\qquad(31)$$

where

$$R=f_{uuu}u^3+3f_{uuv}u^2v+3f_{uvv}uv^2+f_{vvv}v^3,\quad S=g_{uuu}u^3+3g_{uuv}u^2v+3g_{uvv}uv^2+g_{vvv}v^3,$$

$$h_1=(P+yQ)-2xyk_T{}^2d_2{}^T,\ \bar{h_2}=2xyk_T{}^2d_2{}^1,$$

$$G_1=-(k_T{}^2yd_2{}^T(xv_0+u_0+xv_{11}+u_{11})+(f_{uu}x+fuv+y(g_{uu}x+g_{uv}))(u_0+u_{11})+$$
$$(f_{uv}x+f_{vv}+y(g_{uv}x+g_{vv}))(v_0-v_{11})+(R+yS),$$

$$G_2=-(k_T{}^2yd_2{}^T(xv_0+u_0+xv^*+u^*)+(f_{uu}x+fuv+y(g_{uu}x+g_{uv}))(u_0+u^*)+$$
$$(f_{uv}x+f_{vv}+y(g_{uv}x+g_{vv}))(v_0-v^*)+(R+yS).$$

The remaining equations can be acquired by the changing of the subscript of W. A_j can be expressed as (for (j=1,2,3))

$$A_j=\varepsilon W_j+\varepsilon^2V_j+O(\varepsilon^3).\qquad(32)$$

We obtain the amplitude equations for W_i, with the help of equation (32), as

$$\tau_0\frac{\partial A_1}{\partial t}=\mu A_1+h\bar{A}_2\bar{A}_3-[g_1|A_1|^2+g_2(|A_2|^2+|A_3|^2)]A_1,\qquad(33)$$

where

$$\tau_0=\frac{x+y}{d_4{}^Tk_T{}^2xy},\quad\mu=\frac{d_4-d_4{}^T}{d_4{}^T},\quad h=\frac{h_1+\mu h_2}{d_4{}^Tk_T{}^2xy},$$
$$h_2=-2xyk_T{}^2d_2{}^1,g_1=\frac{G_1}{d_4{}^Tk_T{}^2xy},\ g_2=\frac{G_2}{d_4{}^Tk_T{}^2xy}.$$

Similarly, the remaining equations can be obtained as

$$\tau_0\frac{\partial A_2}{\partial t}=\mu A_2+h\bar{A}_1\bar{A}_3-[g_1|A_2|^2+g_2(|A_1|^2+|A_3|^2)]A_2,\qquad(34)$$

$$\tau_0\frac{\partial A_3}{\partial t}=\mu A_3+h\bar{A}_1\bar{A}_2-[g_1|A_3|^2+g_2(|A_1|^2+|A_2|^2)]A_3.\qquad(35)$$

5.1 Amplitude stability analysis

Amplitudes in equations (33)–(35) can be broken into segments to modality $v_j=|A_j|$ and respected phase angle φ_j. Now, putting $v_j\exp(i\varphi_j)=A_j$ into (33)–(35) and splitting the real and imaginary parts, we obtain differential equations of real variable as

$$\tau_0\frac{\partial\psi}{\partial t}=-h\frac{v_1{}^2v_2{}^2+v_2{}^2v_3{}^2+v_3{}^2v_1{}^2}{v_1v_2v_3}\sin\varphi,\qquad(36)$$

$$\tau_0\frac{\partial v_1}{\partial t}=\mu v_1+hv_2v_3\cos\varphi-g_1v_1{}^3-g_2(v_2{}^2+v_3{}^2)v_1,\qquad(37)$$

$$\tau_0\frac{\partial v_2}{\partial t}=\mu v_2+hv_3v_1\cos\varphi-g_1v_2{}^3-g_2(v_3{}^2+v_1{}^2)v_2,\qquad(38)$$

$$\tau_0\frac{\partial v_3}{\partial t}=\mu v_3+hv_1v_2\cos\varphi-g_1v_3{}^3-g_2(v_1{}^2+v_2{}^2)v_2,\qquad(39)$$

here, $\varphi=\varphi_1+\varphi_2+\varphi_3$.

The above mathematical model holds five types of solutions based upon the equilibrium of the system

1.The equilibrium point is given by

$v_1=v_2=v_3=0$,

is stable equilibrium if $\mu<\mu_2=0$ and unstable equilibrium if $\mu>\mu_2=0$.

2.Strip spatial patterns given by

$$v_1=\sqrt{\frac{\mu}{g_1}}\neq0,\ v_2=v_3=0$$

is stable if $\mu>\mu_3=\frac{h^2g_1}{(g_2-g_1)^2}$ and unstable if $\mu<\mu_3$.

3.Spot spatial patterns given by

$$v_1=v_2=v_3=\frac{|h|\pm\sqrt{h^2+4(g_1+2g_2)\mu}}{2(g_1+2g_2)},$$

with $\psi=0$ or π, and exist when,

$$\mu>\mu_1=\frac{-h^2}{4(g_1+2g_2)}$$

the solution $v^+ = \frac{|h|+\sqrt{h^2+4(g_1+2g_2)\mu}}{2(g_1+2g_2)}$ is stable if

$$\mu < \mu_4 = \frac{2g_1+g_2}{(g_1+2g_2)^2}h^2,$$

and $v^- = \frac{|h|-\sqrt{h^2+4(g_1+2g_2)\mu}}{2(g_1+2g_2)}$ is unstable.

4.The spot-stipe are given by

$$v_1 = \frac{|h|}{g_2-g_1},\ v_2 = v_3 = \sqrt{\frac{\mu - g_1 {v_1}^2}{g_1+g_2}},$$

with $g_2 > g_1$. This exist when $\mu > \mu_3$ and are always unstable.

6 Results and numerical simulations

Here we employ numerical simulations to confirm the theoretical consequences obtained in the previous sections. This will likewise assist us with understanding the impacts of self-diffusion on spatial pattern formation by the model (3). The computer simulation has been carried out with the parameters $h_1 = 0.01$, $N = 1.2$, $\sigma = 10.0$, and consider diffusion (d) and cooperation rate coefficients as controlling parameters. The non-trivial equilibrium states are (0, 0), (1.2, 0), (0.7638, 2.7763) and (0.6875, 2.9362) using above parameter values. Equilibrium state (0.6875, 2.9362) is stable and (0.7638, 2.7763) is unstable. Hence, ubiquitously our focus on the spatial aspect of the system, we have contemplated about the stable equilibrium point (0.6875, 2.9362). The time evolution of prey and predator in the non-spatial zone is shown in Figure 1. Observe that the dimensionless parameter $N = \frac{e\lambda}{m}K$, including of the death rate of predators, carrying capacity, conversion efficiency and the attack rate, which is described as the mean number of descendant produced from a individual predator throughout its life, when proposed within the population of prey at carrying efficiency. If $N = 1.2$ and the cooperation coefficient α (= 0.1, 0.5) is small, then the population of predator go to extinct as the population of prey is too small to sustain them (see Figures 1(a,b)). However, for large value of α (= 0.6, 0.7, 0.8), the predator survives due to hunting cooperation behavior in predators (see Figures 1(a,b)). Figure 2 shows the bifurcation diagram for prey and predator species density with α as the bifurcation parameter. We start by differing the pace of hunting cooperation α (see Figure 2). The predator extinct steady state is stable for possible numerics of the parameter α (red curves). For few numeric values of α, a Hopf-bifurcation take place (α = 0.7671) that is the stable non-trivial steady state becomes unstable so that stable limit cycle oscillations appears, and notice that amplitudes rapidly grows with α.

We carry out entire computer simulations of the system (3) over the positive introductory population distribution and Neumann conditions, in 2-D spatial space. The simulation space size is 100×100 with time-step $= 0.001$ (Δt) and space-step $= 0.5$ ($\Delta x = \Delta y$). The parameters σ, N and h_1 remain the same ($\sigma = 10$, $N = 1.2$, $h_1 = 0.01$) and α is used as the control parameter (likewise non-spatial case).

We presently exhibit Turing instability (diffusion-driven instability) and the corresponding spatial patterns for model (3). Albeit, the Turing instability's conditions has been obtained theoretically in prevenient section, whether these conditions are satisfied with the parameter values, is yet to be examined. Now, we draw the graph of Turing instability stipulation (12) for different values of diffusion coefficients (d) (remaining parameters are fixed, specifically, $h_1 = 0.01$, $\alpha = 0.55$,

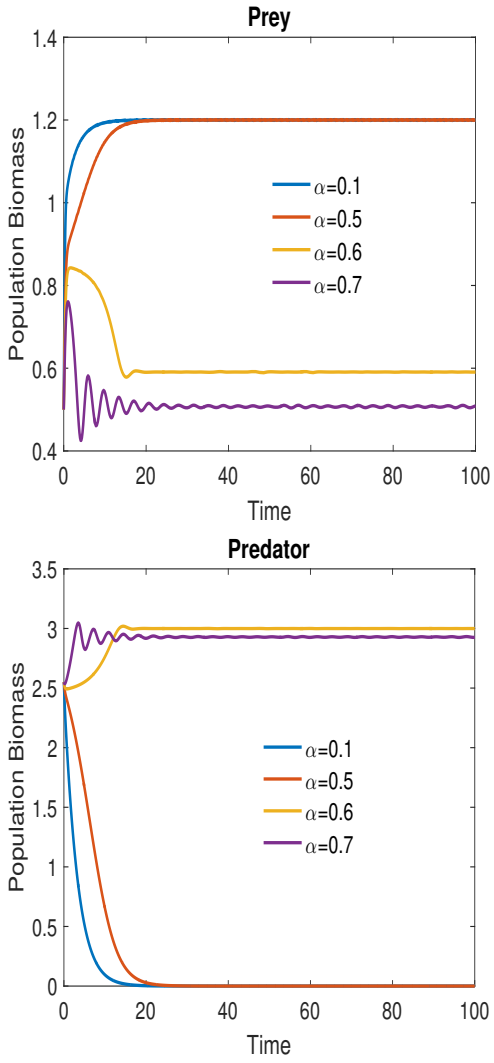

Fig. 1: Time evolution of (a) prey and (b) predator in the non-spatial domain of the model for fixed parameters $\sigma = 10.0$, $N = 1.2$, $h_1 = 0.01$ and different parameter values of hunting cooperation rate (α) which are mentioned in figures.

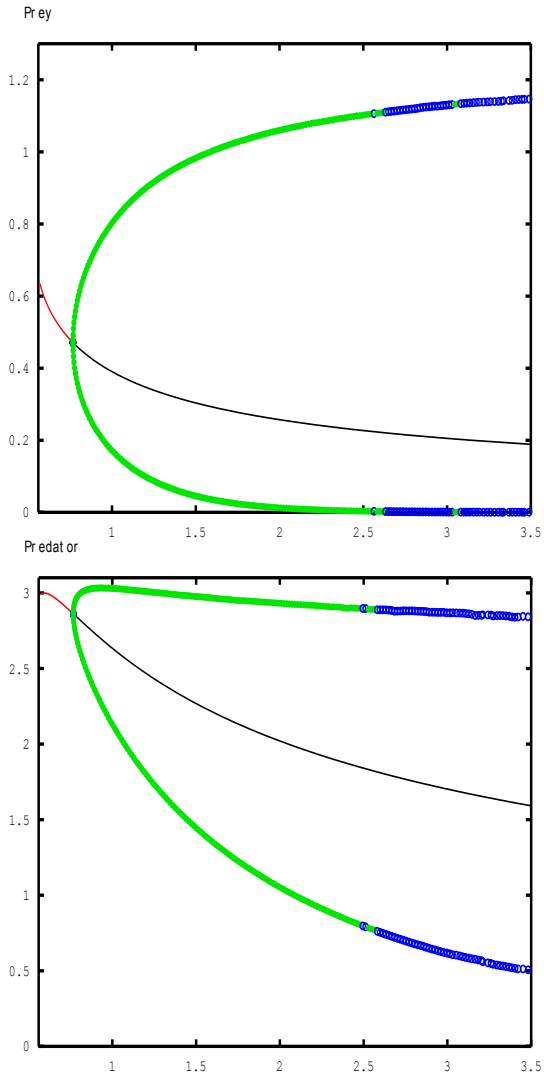

Fig. 2: Bifurcation graph against the hunting cooperation rate (parameter of bifurcation), and the N, σ, h_1 are set at h_1=0.01, σ=10, N=1.2, respectively. Figure 2(a) represents the density of prey (y-axis) vs rate of hunting cooperation α (x-axis), and Figure 2(b) shows the density of predator (y-axis) vs rate of hunting cooperation α (x-axis). Red part of the graph is where the equilibrium point is stable, Gray part of the graph, unstable. Filled green circles shows stable periodic existence branch and blue open circles are unstable, which starts with the Hopf-bifurcation α=0.7671.

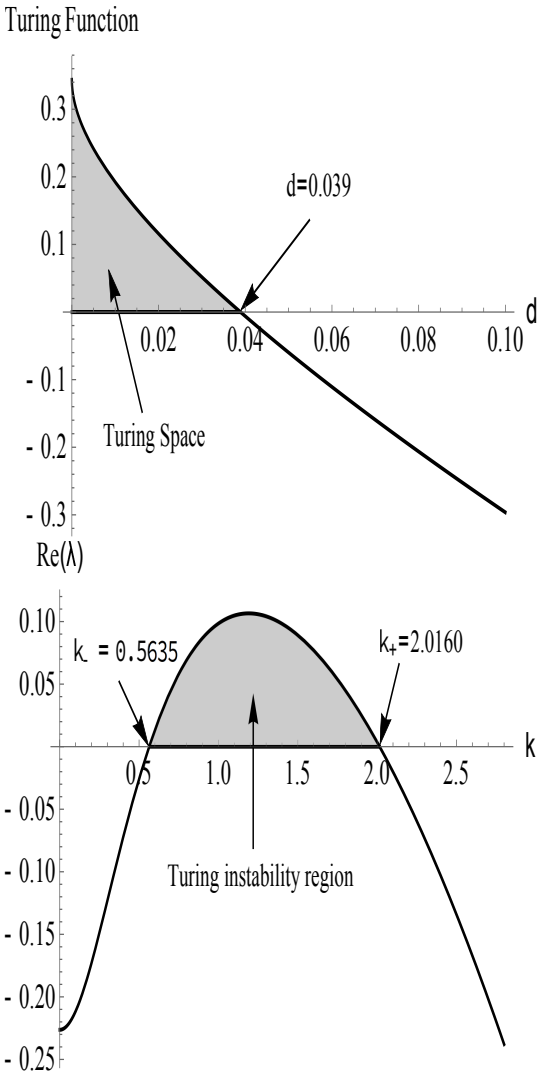

Fig. 3: (a) The region for the origination of pattern formation corresponding to diffusive-driven instability; (b) Proliferation relation for d=30.

$\sigma = 10.0$, $N = 1.2$). Figure 3(a) represents the region for the origination of pattern formation corresponding to diffusive-driven instability stipulation versus the diffusion coefficient (d). We note that the stipulation of the Turing instability, i.e., equation (12) satisfies, when diffusion coefficient is sufficiently small, ending on $d = 0.039$ (see Figure 3(a)). The pattern dispersal graph for the model (3) is represented in Figure 3(b), and the dispersal condition is shown by $Re(\lambda)$ of the diffusive model. The sketch of $Re(\lambda)$ versus the wave-number (k) is represented in Figure 3(b). $Re(\lambda) > 0$ satisfies, the wave-number (k) lies in the span (k_-, k_+), i.e., $(0.5635, 2.0160)$. Moreover, we receive the control parameter zone for diffusive-driven instability via sufficient stipulation, which is represented in Figure 4.

We have represented the mass dispersion of prey and predator in Figure 5 which are three kinds of spatiotemporal patterns namely spot, spot-stripe and stripe. Figures 5(a) and 5(d) exhibit the 2-D spots stripe patterns of the model (3) at time t = 2000 (2,000,000 iterations) and α = 0.55 with $d = 0.023$. Note that the hexagonal diffusive-driven patterns persist over the overall dwelling eventually (see Figures 5(a) and 5(d)). In Figure 5(a), we can noticed that the minimal density of

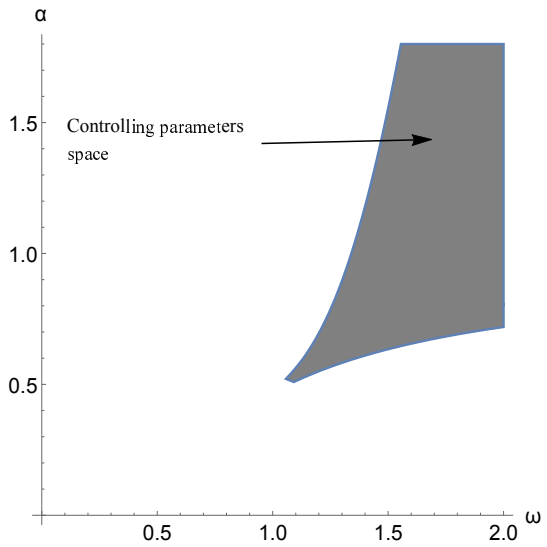

Fig. 4: Space for diffusive-driven instability corresponding to Turing stipulation.

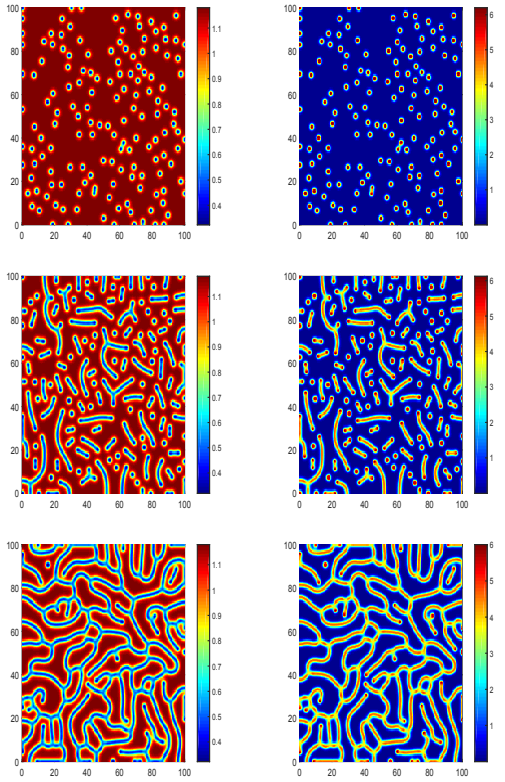

Fig. 5: Spatial population distribution of the prey (left column) and predator (right column) at time moment $t = 2000$ $(2,000,000$ iterations) for distinct cooperation rate (α) with initial distribution. **(a)** & **(d)** $\alpha = 0.55$; **(b)** & **(e)** $\alpha = 0.56$; **(c)** & **(f)** $\alpha = 0.57$. Remaining numeric values are $h_1 = 0.01$, $N = 1.2$, $\sigma = 10$, $d = 0.023$.

prey (blue-spot) are scattered on a red simulated domain (maximum density of prey), i.e., the preys are dispersed with low density. On the contrary, Figure 5(d) comprises of red hexagonal patterns on a blue simulated space, viz, the population of predators are segregated with high mass. As the α is increased to 0.56, few hexagonal patterns broken into stripes resulting in spots-stripe spatial in both prey and predator population (see Figures 5(b) and 5(e)). As α is increased to 0.57, the spatial behavior of the system represents a decomposition of the spot and origination in stripe spatial pattern only (Figures 5(c) and 5(f)). Therefore, by increasing the control parameter α, a series spot $\rightarrow$ spot-stripe $\rightarrow$ stripe is noticed.

We exhibit the pattern formation of the density of prey and predator concerning various diffusion coefficient rates d (see Figure 6). Figure 6(a) and 6(d) demonstrate the 2-D diffusive pattern formation of the system (3) at time t = 2000 (2,000,000 iterations) with diffusion rate d = 0.0175 for the prey and predator. Note that the stripe diffusive-driven patterns prevail over the overall dwelling eventually. In Figure 6(a), it is notice that minimum density of prey (blue stripes) are spreads on a red simulated zone (maximum density of prey). On the other hand, Figure 6(d) consists of red stripes on a blue background. As the diffusion rate d is increases to 0.02, some stripes split into spots resulting in spots-stripes patterns in both prey and predator population (Figures 6(b), 6(e)). When d is increases to 0.028, the dynamics of the model exhibits a decay in the stripes and emergence in spots pattern (see Figures 6(c), 6(f)). A sequence stripes $\rightarrow$ spot-stripes $\rightarrow$ spots is obtained, when we have increased the value of d (rate of diffusion).

7 Conclusions

In mathematical biology, a comprehensive framework for the study of the spatial pattern formation, in systems of interacting inhabitants, has eternally a focus of attraction, as their knowledge aides to magnify the knowing of predator–prey models. We have analyzed a spatiotemporal predator–prey system with hunting cooperation in predators and type-III functional response under favorable initial population distribution and Neumann boundary limitations. We have proposed an extensive analysis for temporal and spatiotemporal systems and considered feasible framework of pattern formation in the spatiotemporal predator–prey system. While investigating the spatial predator–prey system, firstly, we obtained the condition for Turing bifurcation and then recognized the respected space for diffusive-driven spatial pattern formation. In our study, we have used the coefficient of hunting cooperation in predators and the coefficient of diffusion as the controlling parameters. Utilizing the numerical values of the parameters from the diffusive-driven space (Turing

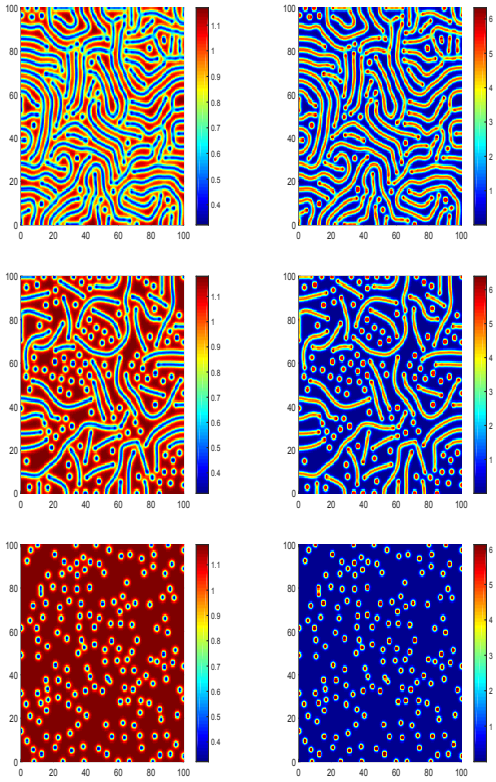

Fig. 6: Spatial population distribution of the prey (left column) and predator (right column) at time moment $t = 2000$ ($2,000,000$ iterations) for distinct diffusion coefficient (d) with initial distribution. **(a)** & **(d)** $d = 0.0175$; **(b)** & **(e)** $d = 0.02$; **(c)** & **(f)** $d = 0.028$. Remaining numeric values are $h_1 = 0.01$, $N = 1.2$, $\sigma = 10$, $\alpha = 0.55$.

space), we examine the qualitative characteristics of the system by the series of numerical simulations.

Our numerical computation of the model has been classified into two distinct areas, to be specific, the non-spatial and the spatial spaces. We have emphasized the impact of predators's hunting cooperation alongside the carrying capacity of the predators. After numerical computation, we affirm that in the temporal space, for specific N, the amplification in the hunting cooperation in the predators, support them to persevere. For specific N, the hunting cooperation in predators perform a critical job in the co-existence of populations in spatial domain. By changing the coefficient of cooperation, we obtain different kinds of spatial patterns, in particular, spots, stripes, and spots-stripes. We can see that there exist spot kind spatial patterns for prey. It implies that the preys are isolated by low density, and the rest part of the simulated space is highly dense, implies that the preys have separated in lowly dense clusters over the sizeable simulated zone and are protected. Likewise, spatial spot pattern formation in predators conveys that the predators are separated and scattered yet still survive. Massive African predators like Acinonyx jubatus, Panthera pardus, and Panthera leo consistently originate ungulates, twofold their mass with the chance of injury or demise to the predator during prey catch but can easily be overcome by cooperative hunting, that can increase hunting success rate [33].

Strategies and results in the paper may intensify the methodical investigation of spatial patterns development in the predator–prey model, and may finely uphold in few extraordinary research measurements. Further investigation is essential to study the behavior of the spatial patterns of other ecological models. It is worth mentioning that the study of the movement of the biological species in the diffusive predator–prey systems under hunting cooperation is a significant concept. This work highlights a number of research areas for future consideration in spatial pattern formation.

Acknowledgement

Research of the first author was supported by the Graphic Era Hill University Dehradun.

Conflicts of Interest

The authors declare that there is no conflict of interest regarding the publication of this article.

References

[1] V. Ardizzone, P. Lewandowski, M.H. Luk, Y.C. Tse, N.H. Kwong, A. Lücke, M. Abbarchi, E. Baudin, E. Galopin, J. Bloch, A. Lemaitre, P.T. Leung, P. Roussignol, R. Binder, J. Tignon and S. Schumacher, Formation and control of Turing patterns in a coherent quantum fluid, *Sci. Rep.*, **3**, 1–6 (2013).

[2] J.D. Murray, *Mathematical Biology II: Spatial Models and Biomedical Applications*, Springer, Berlin (2003).

[3] L.A. Segel and J.L. Jackson, Dissipative structure: an explanation and an ecological example, *J. Theor. Biol.*, **37**, 545–559 (1972).

[4] U. Dieckmann, R. Law and J.A.J. Metz, *The Geometry of Ecological Interactions: Simplifying Spatial Complexity*, Cambridge University Press, Cambridge (1988).

[5] S.A. Levin and L.A. Segel, Hypothesis for origin of planktonic patchiness, *Nature*, **259**, 659–659 (1976).

[6] P.K. Maini, D.L. Benson and J.A. Sherratt, Pattern formation in reaction–diffusion models with spatially inhomogeneous diffusion coefficients, *Math. Med. Biol.*, **9**, 197–213 (1992).

[7] G.R. Shaver, *Spatial heterogeneity: Past, present, and future, in Ecosystem Function in Heterogeneous Landscapes*, Springer, Berlin (2005).

[8] F. Vinatier, P. Tixier, P.F. Duyck and F. Lescourret, Factors and mechanisms explaining spatial heterogeneity: A review of methods for insect populations, *Methods Ecol. Evol.*, *2*, 11–22 (2011).

[9] H. Malchow, S.V. Petrovskii and E. Venturino, *Spatiotemporal Patterns in Ecology and Epidemiology: Theory, Models, and Simulation*, Chapman and Hall/CRC (2008).
[10] A. Okubo and S.A. Levin, *Diffusion and Ecological Problems: Modern Perspectives*, Springer, Berlin (2013).
[11] A.B. Medvinsky, S.V. Petrovskii, I.A. Tikhonova, H. Malchow and B.L. Li, Spatiotemporal complexity of plankton and fish dynamics," *SIAM Rev.*, **44**, 311–370 (2002).
[12] A.M. Turing, The chemical basis of morphogenesis, *Phil. Trans. Royal Soc. B: Biol. Sci.*, **237**, 37–72 (1952).
[13] R.A. Barrio, C. Varea, J.L. Aragón and P.K. Maini, A two–dimensional numerical study of spatial pattern formation in interacting Turing systems, *Bull. Math. Biol.*, **61**, 483–505 (1999).
[14] H.P. Greenspan, Models for the growth of a solid tumor by diffusion, *Stud. Appl. Math.*, **51**, 317–340 (1972).
[15] A. Matzavinos, M.A. Chaplain and V.A. Kuznetsov, Mathematical modeling of the spatiotemporal response of cytotoxic T–lymphocytes to a solid tumour, *Math. Med. Biol.*, **21**, 1–34 (2004).
[16] M. Papadogiorgaki, P. Koliou, X. Kotsiakis and M.E. Zervakis, Mathematical modelling of spatiotemporal glioma evolution, *Theor. Biol. Med. Model.*, **10**, 1–47 (2013).
[17] X.C. Zhang, G.Q. Sun and Z. Jin, Spatial dynamics in a predator–prey model with Beddington-DeAngelis functional response, *Phys. Rev. E.*, **85**, 021924 (2012).
[18] Q.Q. Zheng and J.W. Shen, Dynamics and pattern formation in a cancer network with diffusion, *Comm. Nonlinear Sci. Numer. Simul.*, **27**, 93–109 (2015).
[19] F. Courchamp, L. Berec and J. Gascoigne, *Allee Effects in Ecology and Conservation*, Oxford University Press, Oxford (2008).
[20] P.A. Stephens and W.J. Sutherland, Consequences of the Allee effect for behaviour, ecology and conservation, *Trends Ecol. Evol.*, **14**, 401–405 (1999).
[21] P.A. Stephens, W.J. Sutherland and R.P. Freckleton, What is the Allee effect?, *Oikos*, **87**, 185–190 (1999).
[22] F. Courchamp, T. Clutton-Brock and B. Grenfell, Inverse density dependence and the Allee effect, *Trends Ecol. Evol.*, **14**, 405–410 (1999).
[23] E. González-Olivares, H. Meneses-Alcay, B. González-Yañez, J. Mena-Lorca, A. Rojas-Palma and R. Ramos-Jiliberto, Multiple stability and uniqueness of the limit cycle in a Gause-type predator–prey model considering the Allee effect on prey, *Nonlinear Anal. Real World Appl.*, **12**, 2931–2942 (2011).
[24] A.Y. Morozov, S.V. Petrovskii and B.L. Li, Bifurcations and chaos in a predator–prey system with the Allee effect, *Proceed. Royal Soc. B: Biol. Sci.*, **271**, 1407–1414 (2004).
[25] J. Wang, J. Shi and J. Wei, Dynamics and pattern formation in a diffusive predator–prey system with strong Allee effect in prey, *J. Diff. Equ.*, **251**, 1276–1304 (2011).
[26] J. Wang, J. Shi and J. Wei, Predator–prey system with strong Allee effect in prey, *J. Math. Biol.*, **62**, 291–331 (2011).
[27] S.R. Zhou, Y.F. Liu and G. Wang, The stability of predator–prey systems subject to the Allee effects, *Theor. Popul. Biol.*, **67**, 23–31 (2011).
[28] A. Bompard, I. Amat, X. Fauvergue and T. Spataro, Host-parasitoid dynamics and the success of biological control when parasitoids are prone to Allee effects, *PLoS One*, **8**, e76768 (2013).
[29] A.M. de Ross, L. Persson and H.R. Thieme, Emergent Allee effects in top predators feeding on structured prey populations, *Proceed. Royal Soc. B: Biol. Sci.*, **270**, 611–618 (2003).
[30] A. Verdy, Modulation of predator–prey interactions by the Allee effect, *Ecol. Model.*, **221**, 1098–1107 (2010).
[31] M.T. Alves and F.M. Hilker, Hunting cooperation and Allee effects in predators, *J. Theor. Biol.*, **419**, 13–22 (2017).
[32] L. Berec, Impacts of foraging facilitation among predators on predator–prey dynamics, *Bull. Math. Biol.*, **72**, 94–121 (2010).
[33] H.S. Clements, C.J. Tambling and G.I.H. Kerley, Prey morphology and predator sociality drive predator–prey preferences, *J. Mammal.*, **97**, 919–927 (2016).